THE JOURNAL OF BIOLOGICAL CHEMISTRY VOL. 291, NO. 12, pp. 6494–6506, March 18, 2016
© 2016 by The American Society for Biochemistry and Molecular Biology, Inc. Published in the U.S.A.

Regulation of Phagolysosomal Digestion by Caveolin-1 of the Retinal Pigment Epithelium Is Essential for Vision*

Received for publication, August 20, 2015, and in revised form, January 23, 2016 Published, JBC Papers in Press, January 26, 2016, DOI 10.1074/jbc.M115.687004

Saumil Sethna[‡1], Tess Chamakkala[‡], Xiaowu Gu[§], Timothy C. Thompson[¶], Guangwen Cao[¶2], Michael H. Elliott[§3], and Silvia C. Finnemann[‡4]

From the [‡]Department of Biological Sciences, Center for Cancer Genetic Diseases and Gene Regulation, Fordham University, Bronx, New York 10458, the [§]Department of Ophthalmology, University of Oklahoma Health Sciences Center, Oklahoma City, Oklahoma 73104, and the [¶]Department of Genitourinary Medical Oncology, University of Texas M.D. Anderson Cancer Center, Houston, Texas 77030

Caveolin-1 associates with the endo/lysosomal machinery of cells in culture, suggesting that it functions at these organelles independently of its contribution to cell surface caveolae. Here we explored mice lacking caveolin-1 specifically in the retinal pigment epithelium (RPE). The RPE supports neighboring photoreceptors via diurnal phagocytosis of spent photoreceptor outer segment fragments. Like mice lacking caveolin-1 globally, $^{RPE}CAV1^{-/-}$ mice developed a normal RPE and neural retina but showed reduced rod photoreceptor light responses, indicating that lack of caveolin-1 affects photoreceptor function in a non-cell-autonomous manner. $^{RPE}CAV1^{-/-}$ RPE *in situ* showed normal particle engulfment but delayed phagosome clearance and reversed diurnal profiles of levels and activities of lysosomal enzymes. Therefore, eliminating caveolin-1 specifically impairs phagolysosomal degradation by the RPE *in vivo*. Endogenous caveolin-1 was recruited to maturing phagolysosomes in RPE cells in culture. Consistent with these *in vivo* data, a moderate increase (to ~2.5-fold) or decrease (by half) of caveolin-1 protein levels in RPE cells in culture was sufficient to accelerate or impair phagolysosomal digestion, respectively. A mutant form of caveolin-1 that fails to reach the cell surface augmented degradation like wild-type caveolin-1. Acidic lysosomal pH and increased protease activity are essential for digestion. We show that halving caveolin-1 protein levels significantly alkalinized lysosomal pH and decreased lysosomal enzyme activities. Taken together, our results reveal a novel role for intracellular caveolin-1 in modulating phagolysosomal function. Moreover, they show, for the first time, that organellar caveolin-1 significantly affects tissue functionality *in vivo*.

Support of the neural retina generally and of adjacent photoreceptor neurons specifically by the retinal pigment epithelium (RPE)[5] is essential for vision (1). A major function of the RPE is its contribution to photoreceptor outer segment renewal, a continuous and life-long rejuvenation process that involves the formation of new membrane disks at the proximal end of the outer segment and diurnal shedding of distal spent outer segment tips (2). Outer segment renewal is critical for photoreceptor function and survival, and any abnormality is thought to impair vision. RPE cells participate in outer segment renewal by clearing shed photoreceptor outer segment fragments (POS) by receptor-mediated phagocytosis (3).

Mechanistically, RPE phagocytosis belongs to a family of conserved non-inflammatory clearance phagocytosis pathways that other cell types use to remove apoptotic cells and debris. These pathways have in common that their failure to efficiently clear debris contributes to human disease. However, unlike other forms of phagocytosis, RPE clearance of POS occurs in a strict diurnal rhythm that is regulated by light and circadian mechanisms (4). This is a unique advantage for RPE phagocytosis studies because all steps of the synchronized phagocytic process may be quantified precisely *in situ* in the intact, undisturbed retinas of experimental animals. Content in the RPE of engulfed rod POS phagosomes peaks shortly after light onset and declines characteristically within several hours as RPE cells complete digestion of their phagocytic load before the next burst of intake (5).

Like other phagocytic pathways, ingested phagosomes in the RPE fuse with lysosomal vesicles to form phagolysosomes. In POS phagolysosomes, degradation of opsin, which constitutes ~85% of POS protein, requires the aspartic protease cathepsin D and phagosomal acidification (6, 7). Because RPE cells are post-mitotic in the mammalian eye and ingest numerous POS daily, prompt and complete POS engulfment is essential to prevent gradual buildup of undigested debris in the RPE (8). Inefficient RPE lysosomal function causes accumulation of debris in human and experimental animal RPE that can be toxic and

* This study was supported by National Institutes of Health Grants R01EY013295 (to S. C. F.) and R01EY019494 (to M. H. E.) and Core Grant P30EY021725 and by an unrestricted grant from Research to Prevent Blindness, Inc. (to the Department of Ophthalmology, University of Oklahoma Health Science Center). The authors declare that they have no conflicts of interest with the contents of this article. The content is solely the responsibility of the authors and does not necessarily represent the official views of the National Institutes of Health.

[1] Supported by a Fordham Graduate School of Arts and Sciences alumni dissertation fellowship.

[2] Present address: Dept. of Epidemiology, Second Military Medical University, Shanghai 200433, China.

[3] To whom correspondence may be addressed: Dept. of Ophthalmology, Dean McGee Eye Institute, University of Oklahoma Health Sciences Center, 608 Stanton L. Young Blvd., Oklahoma City, OK 73104. Tel.: 405-271-8001 ext. 30024; E-mail: michael-elliott@ouhsc.edu.

[4] To whom correspondence may be addressed: Dept. of Biological Sciences, Center for Cancer, Genetic Diseases and Gene Regulation, 441 East Fordham Rd., Fordham University, Bronx, NY 10458. Tel.: 718-817-3630; E-mail: finnemann@fordham.edu.

[5] The abbreviations used are: RPE, retinal pigment epithelium/epithelia; POS, photoreceptor outer segment fragments; PFA, paraformaldehyde; ANOVA, analysis of variance; mut, mutant.

contribute to age-related blindness (9–12). Despite its importance, the molecular control of phagolysosomal digestion by the RPE as well as other phagocytic cells remains poorly understood.

The membrane organizer protein caveolin-1 is expressed by the RPE (13) but also by other retinal cell types and the choroidal vasculature (14–16), and global knockout of caveolin-1 impairs rod-driven visual function (17). Caveolins regulate cellular processes by recruiting protein complexes either on the inner leaflet of the plasma membrane or on cytoplasmic organelles (18–20). Interestingly, caveolin-1 on a subset of early endosomes has recently been suggested to influence the fate and signaling of internalized TGF-β receptors, suggesting that vesicular caveolin-1 may alter vesicle functionality (21). Here we explore mice manipulated to lack caveolin-1 specifically and solely in the RPE. Strikingly, eliminating caveolin-1 from the RPE alone is sufficient to impair retinal function. Moreover, our studies identify a novel function for caveolin-1 in regulating phagolysosomal acidification and digestive enzyme activity to ensure efficient and complete clearance phagocytosis.

Experimental Procedures

Antibodies—Primary antibodies used were as follows: α-β-tubulin (Abcam, Cambridge, MA), β-actin (Sigma), caveolin-1 and lamp-1 (Cell Signaling Technology, Danvers, MA), cathepsin D (for microscopy, R&D Systems, Minneapolis, MN; for immunoblotting, Novus Biologicals, Littleton, CO), opsin N terminus clone B6-30 (a gift from Paul Hargrave, University of Florida, Gainesville, FL) (22), opsin N terminus clone Ret-P1 and opsin C terminus clone 1D4 (Millipore, Billerica, MA), transducin (Santa Cruz Biotechnology, Santa Cruz, CA), and transferrin receptor (Life Technologies). Horseradish peroxidase- or Alexa Fluor-conjugated secondary antibodies were from Jackson ImmunoResearch Laboratories (West Grove, PA) and Life Technologies, respectively.

Animals, Tissue Harvest, and Processing—All procedures involving animals were performed according to the Association for Research in Vision and Ophthalmology Statement for the Use of Animals in Ophthalmic and Vision Research and the National Institutes of Health Guide for the Care and Use of Laboratory Animals and were reviewed and approved by the Institutional Animal Care and Use Committees of the University of Oklahoma Health Sciences Center and Fordham University.

$^{RPE}CAV1^{-/-}$ mice were generated by crossing mice expressing Cre in a doxycycline-inducible fashion under the control of the RPE-specific *VMD2* promoter (23, 24) to mice carrying a floxed *CAV1* gene (16, 25). Mice were in the C57BL6 background and were screened and found not to carry the rd8 mutation. RPE-specific Cre expression was induced by feeding pregnant dams a doxycycline-supplemented diet (Bio-Serv, Flemington, NJ) *ad libitum*. The doxycycline diet was provided until weaning, at which point weanlings were transferred to standard mouse chow. Our mating strategy allowed us to generate $^{RPE}CAV1^{+/+}$ and $^{RPE}CAV1^{-/-}$ from the same litters by crossing homozygous floxed, Cre-carrying males with homozygous floxed, Cre-negative females. Therefore, all offspring were exposed to doxycycline, but only Cre expressors displayed recombination of the floxed allele. Mice were housed under a strict 12:12 h light on/off cycle and fed a standard mouse diet (after weaning) and water *ad libitum*. Mice were euthanized by CO_2 asphyxiation before immediate eye enucleation. Eyes were immersion-fixed in Davidson's fixative (33% ethanol, 22% formalin, and 11.5% acetic acid) or in 4% paraformaldehyde (PFA) for paraffin embedding or in 4% PFA in PBS with 1 mM $MgCl_2$ and 0.1 mM $CaCl_2$ (PBS-CM) for Optimal Cutting Temperature compound (OCT) embedding and cryopreservation. Sections from paraffin-embedded eyes were cut on a microtome, mounted on glass slides, and deparaffinized before labeling with hematoxylin and eosin (both from Millipore) for light microscopy or with antibodies for immunofluorescence microscopy. Frozen sections were cut on a cryostat before antibody labeling and immunofluorescence microscopy. Whole mounts of posterior, retina-free eye cups were prepared by dissecting neural retinas from fresh eyes, followed by making radial cuts to flatten the eye cup, fixation in 4% PFA in PBS-CM, and antibody labeling for fluorescence microscopy. For assays requiring tissue extracts, enucleated mouse eyes were opened to remove the lens, the neural retina was dissected from posterior eye cups from select eyes, and the resulting eye tissues were frozen at −80 °C before lysis.

Electroretinography—Electroretinograms were recorded as described previously (17, 23) with slight modifications. Briefly, overnight, dark-adapted mice were anesthetized with ketamine (100 mg/kg) and xylazine (10 mg/kg), and pupils were dilated with 0.5% atropine and 2.5% phenylephrine. Gold wire electrodes were placed on the cornea, a reference electrode in the mouth, and a ground electrode in the tail. To assess rod-driven responses, increasing scotopic stimuli were presented sequentially (−3.7 to 2.6 log scotopic candela (cd)·s/m^2) using a Colordome Espion electroretinography recording system (Diagnosys, Lowell, MA) (26).

Cell Culture, Adenoviral Infection, and Lentivirus-mediated shRNA Knockdown—Rat RPE-derived, immortalized RPE-J cells (ATCC, Manassas, VA) were maintained at 32 °C and 8% CO_2 in DMEM supplemented with 4% FBS (CELLect Gold, ICN, Irvine, CA) and subcultured every 7 days. Post-confluent differentiated cells were used for experiments 6 days after plating (27, 28). For microscopy, cells were either fixed with ice-cold methanol or with 4% PFA in PBS-CM. PFA-fixed cells were permeabilized with 0.2% Triton X-100 in PBS-CM before antibody labeling.

Expression plasmids encoding WT caveolin-1-myc and the scaffolding mutant mut-caveolin-1-myc (F92A, V94A) (29) (a gift from Dr. Patricio Meneses, Fordham University, Bronx, NY) were used to generate replication-defective, recombinant adenoviruses (Welgen, Worcester, MA). The β-galactosidase control adenovirus was purchased from Cell Biolabs (San Diego, CA). Adenoviruses were diluted in serum-free DMEM before addition to confluent RPE-J cells 4 days after plating. After overnight infection, cells were incubated in complete growth medium for a further 24 h before experiments. Replication-deficient lentiviral particles encoding either a scrambled shRNA sequence that will not lead to degradation of any known cellular mRNA (catalog no. sc-108080) or a mixture of three to five target-specific 19- to 25-nucleotide (plus hairpin) silencing

shRNA sequences targeting caveolin-1 (catalog no. sc-106996-V) were purchased from Santa Cruz Biotechnology. RPE-J cells were infected and selected with puromycin according to the protocol of the manufacturer. Entire populations of cells were selected rather than single cell clones to minimize selection of individual clones that had drifted phenotypically from the parental RPE-J cell line.

Synchronized Cell Culture Phagocytosis Assay—POS were purified from fresh porcine eyes obtained from a local slaughterhouse in accordance with an established protocol (30) and used unlabeled or labeled covalently with Alexa Fluor-647 (Life Technologies). For pulse-chase experiments, cells were challenged with 10 POS/cell in serum-free DMEM with 30 nM MFG-E8 for 1 h at 20 °C (pulse, POS binding only) followed by chase for specific time periods with DMEM supplemented with 5% delipidated, heat-inactivated FBS and fixation for microscopy or lysis.

Immunofluorescence Labeling, Lysosome Labeling, and Microscopy—Tissue sections, whole mount eye cup preparations, or fixed cells were labeled with antibodies for fluorescence microscopy. Nuclei were counterstained with DAPI (Life Technologies). For labeling of acidified compartments, RPE-J cells were incubated with 0.1 μM LysoTracker Red DND-99 (Life Technologies) for 15 min at 32 °C. Cells were either imaged live or after they were fixed with 4% PFA for 15 min at room temperature, permeabilized with 0.2% Triton X-100 in PBS-CM for 15 min at room temperature, and co-stained with antibodies. A TSP5 laser-scanning confocal microscopy system (Leica Microsystems, Wetzlar, Germany) was used for image acquisition. Images were further processed and compiled using Adobe Photoshop CS5. For cathepsin D staining or opsin/cathepsin D co-staining, PFA-fixed tissue sections were used. For phagosome counting, paraffin tissue sections were labeled with the opsin antibody B6-30. Stacks of precisely 5-μm thickness were acquired to yield maximal projections showing phagosomes in a constant tissue volume. ImageJ software was used for processing images, and the average number of phagosomes per 100 μm of retina was calculated (described in detail in Ref. 5).

Lysosomal pH Measurement—Lysosomal pH values in cells grown to confluence in 96-well plates were measured using LysoSensor Yellow/Blue DND-160 (Life Technologies) following a published protocol (31). Briefly, cells were loaded with 7.5 μM LysoSensor Yellow/Blue DND-160 for 3 min at 32 °C in DMEM, followed by washing with 20 mM HEPES buffer containing 145 mM KCl, 10 mM dextrose, and 1 mM $MgCl_2$. Cells were incubated further for 5 min before fluorescence measurements using a Spectramax M2E scanner (Molecular Dynamics, Sunnyvale, CA). The excitation/dual emission parameters used were 380 nm and 525/436 nm. The ratio of light emission at 525/436 nm was converted to absolute pH measured according to Guha *et al.* (31). At least three independent experiments were performed with triplicate samples each.

SDS-PAGE and Immunoblotting—Chilled samples were lysed in HNTG buffer (50 mM HEPES, 150 mM NaCl, 10% glycerol, and 1% Triton X-100) with 1× protease inhibitor mixture and 1 mM PMSF (both from Sigma-Aldrich). Clarified lysates were separated using standard protocols for SDS-PAGE, followed by immunoblotting and enhanced chemiluminescence detection (PerkinElmer Life Sciences). Densitometric quantification of immunoblot bands on scanned x-ray films was carried out using ImageJ software (National Institutes of Health, Bethesda, MD).

Quantification of Constitutive Transferrin Receptor Lysosomal Degradation—Transferrin receptor levels were established following exactly the detailed protocol by Matsui and Fukuda (32). Briefly, transferrin receptor levels were quantified by immunoblotting and densitometry, as described above, of lysates obtained from cells treated with 50 μg/ml cycloheximide to stop protein synthesis for various periods of time. Addition of 100 nM bafilomycin A eliminated lysosomal function during treatment in select samples. Decreases in transferrin receptor levels in cycloheximide-treated cells, but not in cells treated with both cycloheximide and bafilomycin A, were interpreted as lysosomal degradation.

Enzyme Assays—For *in vivo* cathepsin D and β-*N*-acetylglucosaminidase activity assessment, mice were euthanized 0.5 or 8 h after light onset. Cathepsin D and β-*N*-acetylglucosaminidase activity was measured in dissected tissue fractions or cells using specific activity assay kits on the basis of synthetic cathepsin D-specific or β-*N*-acetylglucosaminidase-specific fluorogenic substrates following the instructions of the manufacturer (Sigma). Cathepsin D activity was established by directly comparing sample activity to the active cathepsin D standard (Abcam). Enzyme activities were calculated as unit activity per total sample protein content measured using Bradford colorimetric protein quantification.

Data Analysis—All *in vivo* experiments were performed comparing at least four age- and background-matched $^{RPE}CAV1^{+/+}$ and $^{RPE}CAV1^{-/-}$ mice each per assay and per time point where applicable. For cell culture experiments, at least three independent experiments with duplicates or triplicates in each experiment were performed. Student's *t* test or one-way ANOVA with Tukey's post hoc test was used to compare a control sample to test samples, with data presented as mean ± S.E. Differences with $p < 0.05$ were considered significant. Data were analyzed using GraphPad Prism (GraphPad Software, Inc., La Jolla, CA).

Results

Lack of Caveolin-1 Solely in the RPE Impairs Rod-dependent Visual Function—To investigate the contribution of caveolin-1 in the RPE to retinal functionality, we crossed mice expressing doxycycline-inducible Cre recombinase specifically in RPE (24) with mice carrying floxed alleles of caveolin-1 (Fig. 1*A*). Supplying doxycycline to females during pregnancy and until 7 days postnatally resulted in $^{RPE}CAV1^{-/-}$ offspring in which deletion of the floxed allele could be detected in eye cup tissue containing the RPE but not in the retinas from these mice (Fig. 1*B*). Furthermore, reduced levels of caveolin-1 protein specifically in the RPE (Fig. 1, compare *C* and *D*) were observed by immunofluorescence microscopy. Quantification of caveolin-1 in dissected RPE tissue revealed a reduction by 65% on average (Fig. 1, *G* and *H*) in comparison with control mice not carrying the RPE-specific Cre. Control $^{RPE}CAV1^{+/+}$ and induced ^{RPE}-$CAV1^{-/-}$ retinas were morphologically indistinguishable, indicating that doxycycline, Cre, or lack of caveolin-1 did not affect

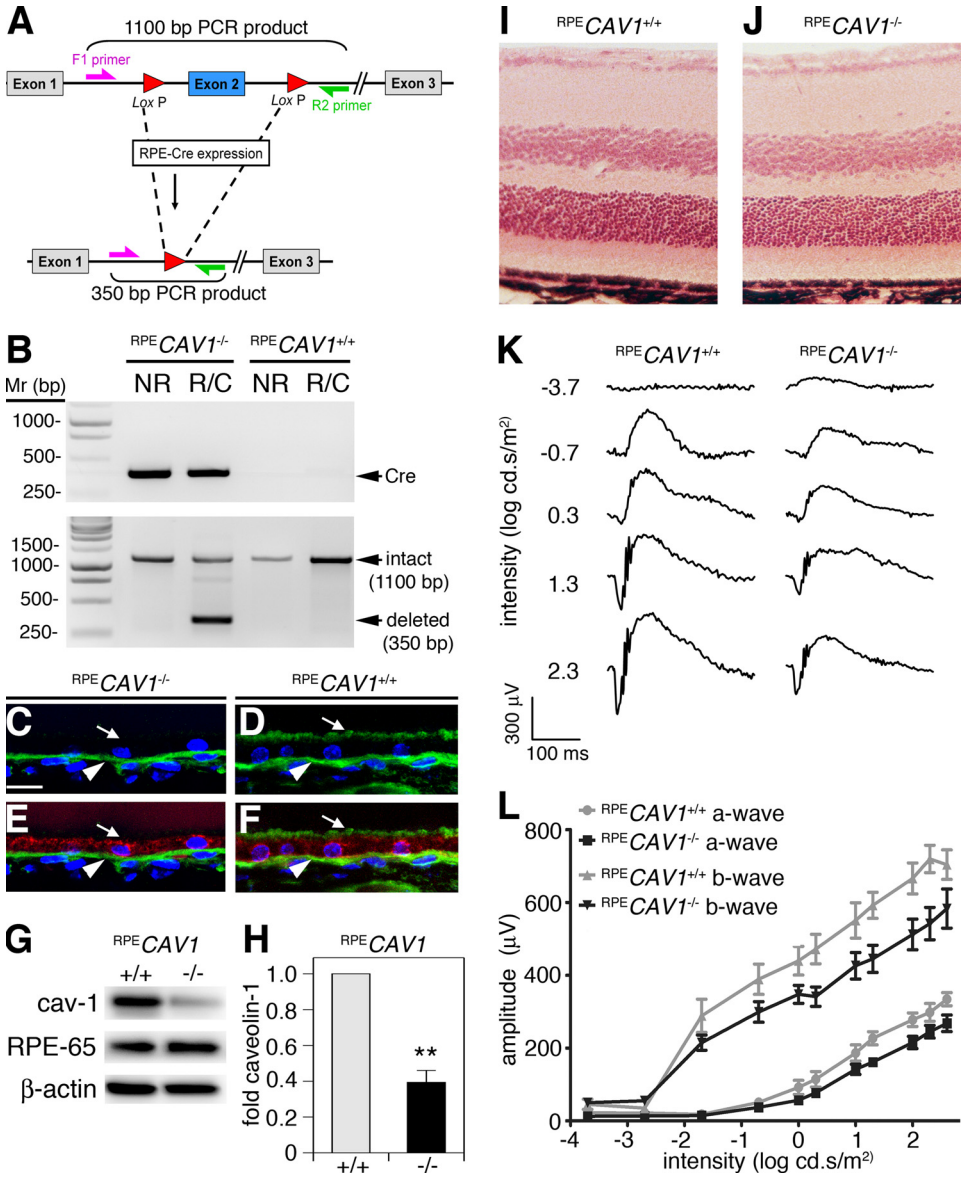

FIGURE 1. **RPE-specific deletion of caveolin-1 impairs rod photoreceptor function but causes no structural damage.** *A*, schematic showing generation of the $^{RPE}CAV1^{-/-}$ mouse. *B*, representative gel of PCR products from genomic DNA from neural retina and RPE/choroid from littermate RPE-Cre-expressing and RPE-Cre-negative mice showing *Cre* (*top panel*) and caveolin-1 floxed product. The 350-bp *CAV1* deletion product (*bottom panel*) is detected only in RPE/choroid from Cre-carrying mice following doxycyline induction. *NR*, neural retina; *R/C*, RPE/choroid. *C–F*, representative images showing cross-sections of RPE/choroid from $^{RPE}CAV1^{-/-}$ (*C* and *E*) and $^{RPE}CAV1^{+/+}$ (*D* and *F*) labeled with caveolin-1 (*green*, *C–F*) and RPE-65 (*red*, *E* and *F*). *Arrows* indicate the apical RPE surface showing the absence or presence of caveolin-1 in $^{RPE}CAV1^{-/-}$ (*C* and *E*) and $^{RPE}CAV1^{+/+}$ (*D* and *F*), respectively. *Arrowheads* indicate the caveolin-1 signal in the choroid. *G*, representative Western blotting analysis showing RPE ablation of caveolin-1 in RPE/choroid lysates from $^{RPE}CAV1^{+/+}$ and $^{RPE}CAV1^{-/-}$ mice. RPE-65 and β-actin are loading controls. *H*, quantification of experimental conditions as mentioned in *G* (**, $p < 0.01$, one sample *t* test). *I* and *J*, representative images showing cross-sections of retinas from $^{RPE}CAV1^{+/+}$ (*I*) and $^{RPE}CAV1^{-/-}$ (*J*) mice stained with hematoxylin, which stains nuclei, and eosin, which stains the extracellular matrix. *K*, representative scotopic electroretinography waveforms from $^{RPE}CAV1^{+/+}$ (*left panel*) and $^{RPE}CAV1^{-/-}$ (*right panel*) mice subjected to the indicated light flash intensities. *L*, intensity/response curves showing a- (*circles*) and b-wave (*triangles*) amplitudes at the indicated light flash intensities. *Gray curves*, $^{RPE}CAV1^{+/+}$ mice; *black curves*, $^{RPE}CAV1^{-/-}$ mice. Data are mean ± S.E. ($n = 7$ mice/group).

retinal development (Fig. 1, compare *I* and *J*). To test whether lack of caveolin-1 in RPE alone affected retinal function, we performed electroretinography. We observed significant reductions in rod photoreceptor responses, as measured by scotopic electroretinography from mice that were dark-adapted overnight (Fig. 1, *K* and *L*). Maximum a-wave amplitudes, a direct measure of rod photoreceptor responses, were reduced significantly in $^{RPE}CAV1^{-/-}$ mice compared with controls from 307 ± 15 μV to 252 ± 19 μV (mean ± S.E., $p < 0.05$, unpaired *t* test). b-Wave amplitudes, a measure of second-order retinal neuronal responses that depend on rod input, were reduced similarly reduced in $^{RPE}CAV1^{-/-}$ mice (Fig. 1, *K* and *L*), from 620 ± 35 μV in $^{RPE}CAV1^{-/-}$ to 481 ± 41 μV (mean ± S.E., $p < 0.05$, unpaired *t* test). Therefore, eliminating caveolin-1 from the RPE has no obvious effect on cell viability and retinal morphology but is sufficient to reduce rod photoreceptor responses to light.

Lack of Caveolin-1 Solely in the RPE Leads to Delayed Phagosome Clearance in Vivo—We hypothesized that photoreceptors may lose function because RPE cells devoid of caveolin-1 fail to

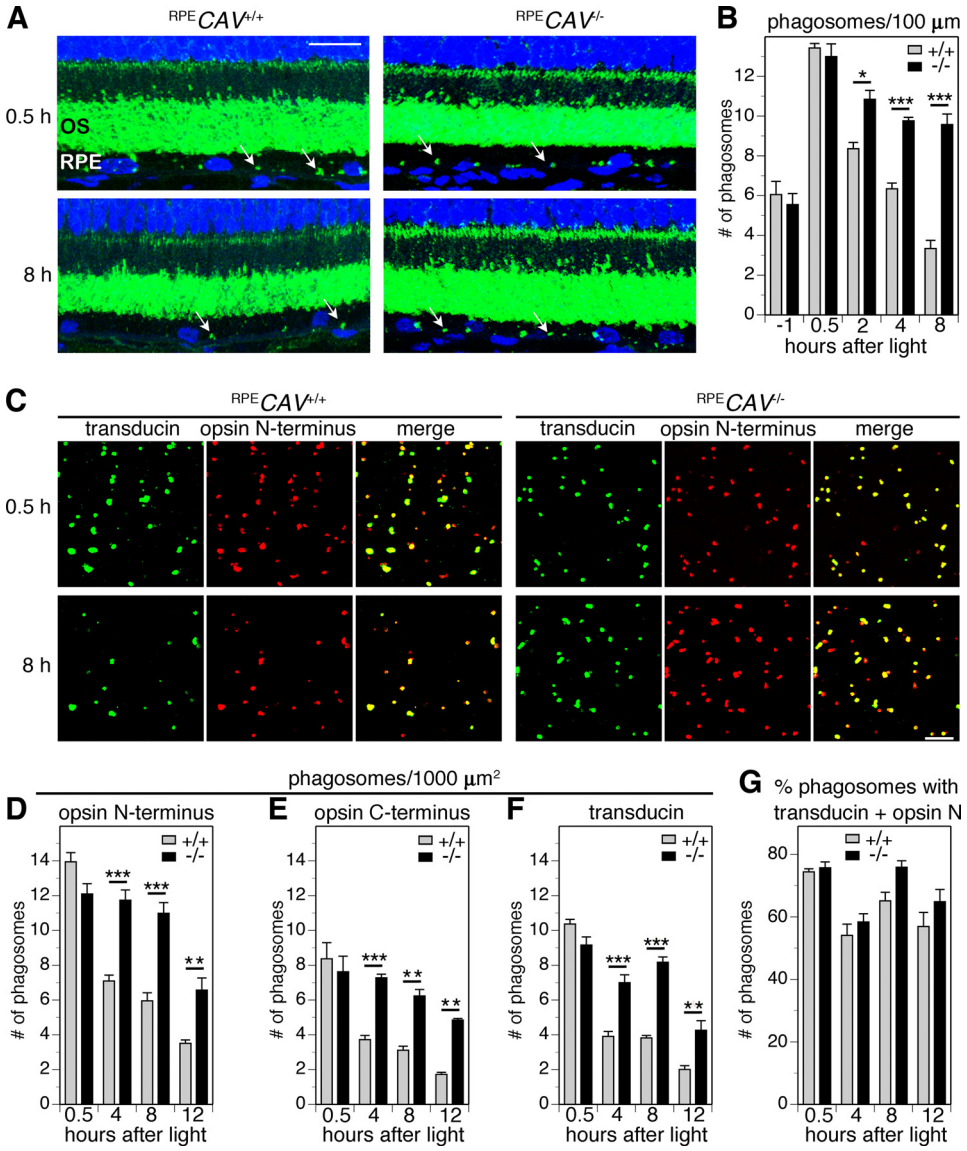

FIGURE 2. **RPE-specific deletion of caveolin-1 impairs POS clearance by RPE cells *in situ*.** *A*, representative images showing cross-sections of retinas from $^{RPE}CAV1^{+/+}$ and $^{RPE}CAV1^{-/-}$ mice, as indicated, sacrificed 0.5 h (*top panels*) or 8 h (*bottom panels*) after light onset, labeled with the opsin N terminus antibody B6-30 (*green*) and nucleic counterstain (*blue*). *Arrows* indicate POS phagosomes residing in the RPE. *OS*, outer segment layer. *Scale bar* = 10 μm. *B*, quantification of the phagosome content of 100-μm stretches of RPE counted from images and samples as shown in *A*. *Error bars* show mean ± S.E. ($n = 4$ mice/group with phagosomes counted in at least 6 images/mouse). *Gray columns*, $^{RPE}CAV1^{+/+}$ mice; *black columns*, $^{RPE}CAV1^{-/-}$ mice. *C*, representative images showing flat mounts of posterior eye cups showing *en face* views of RPE of $^{RPE}CAV1^{+/+}$ and $^{RPE}CAV1^{-/-}$ mice 0.5 h (*top panels*) and 8 h (*bottom panels*) after light onset. Antibodies to transducin (*green*) and opsin N terminus (B6-30) (*red*) label engulfed phagosomes, and the overlay shows phagosomes positive for both proteins (*merge*, *yellow*). *Scale bar* = 10 μm. *D–G*, quantification of phagosomes per 1000 μm² of RPE viewed *en face* at different times after light onset, as indicated, that are positive for opsin-N terminus (*D*), opsin C terminus (*E*), transducin (*F*), or both transducin and opsin N terminus (*G*). *Error bars* show mean ± S.E. of phagosomes counted in images and samples as shown in *C* ($n = 4$ mice/condition, with at least 4 images counted for each staining/mouse). *Gray columns*, $^{RPE}CAV1^{+/+}$ mice; *black columns*, $^{RPE}CAV1^{-/-}$ mice. *, $p < 0.05$; **, $p < 0.01$; ***, $p < 0.001$ for all bar graphs.

fully support outer segment renewal given its requirement for extensive membrane dynamics. The diurnal rhythm of retinal phagocytosis allows quantification of the engulfment and digestion capacity of the RPE by quantifying phagosomes in the RPE *in situ* at specific times in relation to light onset (5). Here we compared phagosome frequency in $^{RPE}CAV1^{+/+}$ and $^{RPE}CAV1^{-/-}$ RPE 0.5, 2, 4, 8, and 12 h after light onset and 1 h before light onset. A similar content of POS marker-positive phagosomes 1 h before and 0.5 h after light onset in these mice suggested that POS shedding and synchronized engulfment take place normally in $^{RPE}CAV1^{-/-}$ mice (Fig. 2, *A* and *B*). However, late in the day, when phagosome numbers in control RPE are low after digestion of the morning phagocytic load, we found phagosome numbers to be abnormally high in $^{RPE}CAV1^{-/-}$ mice (Fig. 2, *A* and *B*). This suggested a defect in POS-opsin digestion rather than engulfment. To assess whether *CAV1* ablation leads to digestion defects for additional POS proteins, we double-labeled RPE whole mount preparations with transducin antibody and with the same opsin antibody as used initially for sections, clone B6-30 raised against the stable rhodopsin N terminus (22). Phagosomes were co-stained for both proteins at both early and late time points, and, as in sections, the phagosome load after light onset was similar in $^{RPE}CAV1^{-/-}$ and $^{RPE}CAV1^{+/+}$ RPE but elevated late in the day

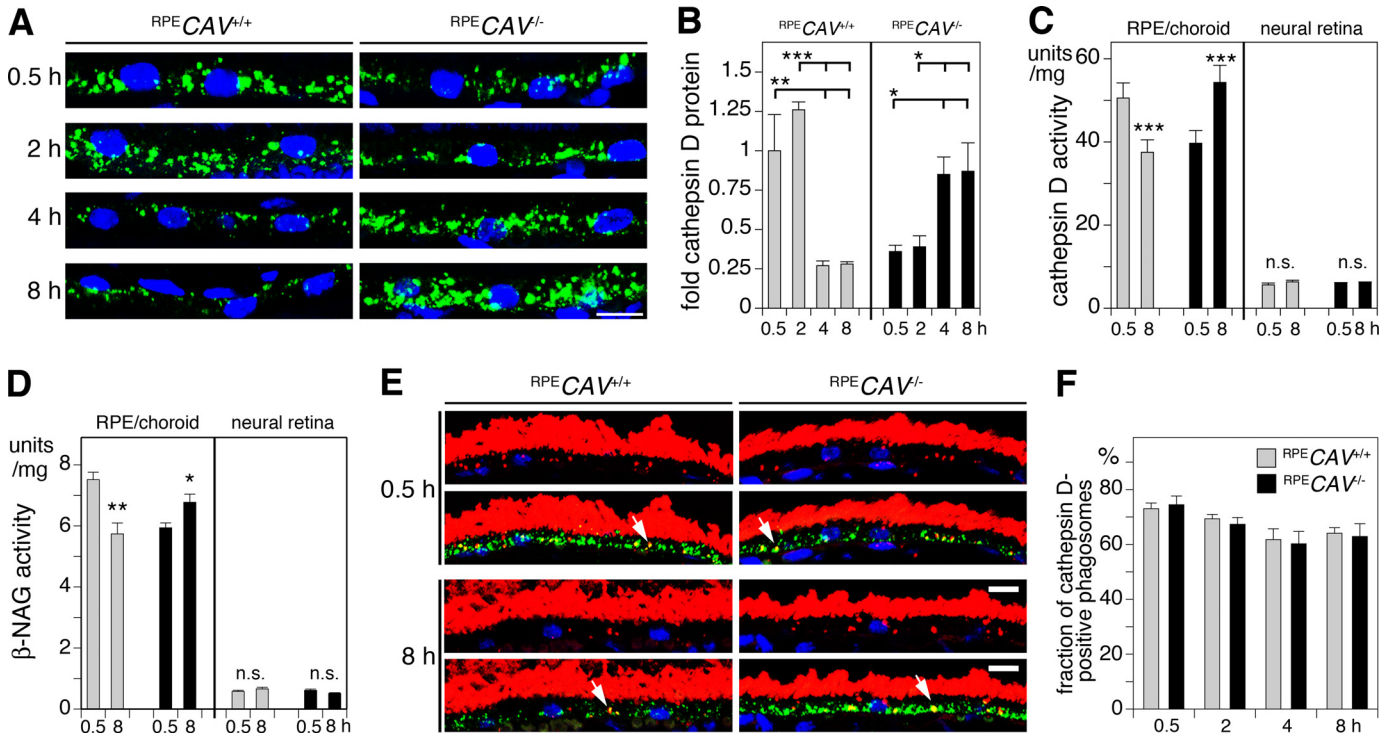

FIGURE 3. **RPE-specific deletion of caveolin-1 reverses the diurnal rhythm in activity of phagolysosomal enzymes in the RPE *in situ*.** *A*, representative images showing close-up views of RPE in retina cross-sections from $^{RPE}CAV1^{+/+}$ and $^{RPE}CAV1^{-/-}$ mice, as indicated, sacrificed between 0.5 and 8 h after light onset, as indicated, labeled with cathepsin D antibody (*green*) and nucleic counterstain (*blue*). *Scale bar* = 10 μm. *B*, quantification of total cathepsin D protein levels in RPE *in situ* from images and samples as shown in *A*. *Error bars* show mean ± S.E. (n = 4 mice/group, with the cathepsin D signal quantified in 4 images/mouse). *Gray columns*, $^{RPE}CAV1^{+/+}$ mice; *black columns*, $^{RPE}CAV1^{-/-}$ mice. *C*, comparison of cathepsin D enzyme activity 0.5 and 8 h after light onset in posterior eye cups enriched in the RPE and neural retina, as indicated from $^{RPE}CAV1^{+/+}$ (*gray columns*) and $^{RPE}CAV1^{-/-}$ mice (*black columns*). *Error bars* show mean ± S.E. (n = 4 mice/condition). *D*, comparison of β-*N*-acetylglucosaminidase enzyme activity in samples as described for *C*. *Error bars* show mean ± S.E. (n = 4 mice/condition). *E*, co-staining of cathepsin D (*green*) with opsin N terminus (*red*) and nuclei (*blue*) in retina cross-sections from $^{RPE}CAV1^{+/+}$ and $^{RPE}CAV1^{-/-}$ mice, as indicated, 0.5 h and 8 h after light onset. *Scale bars* = 10 μm. *F*, quantification of the fraction of phagosomes positive for cathepsin D and opsin in conditions as in *E*. Note that absolute phagosome numbers differ between samples. *Error bars* show mean ± S.E. (n = 4 mice/condition, with at least 4 images/mouse). *Gray columns*, $^{RPE}CAV1^{+/+}$ mice; *black columns*, $^{RPE}CAV1^{-/-}$ mice. *, $p < 0.05$; **, $p < 0.01$; ***, $p < 0.001$; *n.s.*, not significant for all bar graphs.

(Fig. 2*C*). We also labeled phagosomes in whole mounts with antibody against the less stable opsin C terminus (clone ID4 (33, 34)) and found consistent results (Fig. 2*E*). Therefore, regardless of phagosome protein marker, $^{RPE}CAV1^{-/-}$ RPE retained more undigested phagosomes at late time points (Fig. 2, *D–F*). The fraction of transducin and opsin N terminus double-positive phagosomes was similar irrespective of time point or genotype, suggesting an overall defect in phagolysosomal protein digestion (Fig. 2*G*). These *in vivo* data imply that caveolin-1 is not required for phagocytic recognition, binding, or internalization but important for phagolysosomal degradation.

$^{RPE}CAV1^{-/-}$ RPE in Vivo Exhibits Altered Diurnal Regulation of Lysosomal Enzymes but Normal Protease Recruitment to Phagosomes—The activity of the aspartic protease cathepsin D is essential for digestion of POS-opsin (10, 35, 36). To test whether persistent phagosomes in $^{RPE}CAV1^{-/-}$ RPE were due to impaired protease activity, we compared the levels, activity, and recruitment of cathepsin D to phagolysosomes in $^{RPE}CAV1^{+/+}$ and $^{RPE}CAV1^{-/-}$ RPE *in situ*. Immunofluorescence microscopy of cathepsin D in tissue sections revealed higher levels of cathepsin D protein in $^{RPE}CAV1^{+/+}$ RPE during the early phases of phagocytosis, at 0.5 and 2 h, than 4 and 8 h after light onset (Fig. 3, *A* and *B*). The opposite temporal profile was observed for $^{RPE}CAV1^{-/-}$ RPE, with cathepsin D immunoreactivity low at light onset and increasing by 8 h after light onset (Fig. 3, *A* and *B*). Therefore, lack of caveolin-1 leads to a reversal of the diurnal regulation of cathepsin D, likely through a form of organelle load feedback. The molecular mechanisms of this regulation will be a subject of future studies.

Cathepsin D is synthesized as a proform whose enzymatic cleavage in a low pH environment is required for the generation of enzymatically active cathepsin D. Because our antibody staining could not distinguish between inactive and active cathepsin D, we next measured specific enzymatic activity in tissue extracts. To discriminate cathepsin D activity in RPE/choroid and neural retinas, we dissected neural retinas from posterior eye cups before tissue extraction. We found a similar trend for cathepsin D activity as seen for protein levels. Levels of active cathepsin D were elevated in $^{RPE}CAV1^{+/+}$ RPE early after light onset compared with 8 h later, whereas, in $^{RPE}CAV1^{-/-}$ RPE, cathepsin D levels were elevated at 8 h but not immediately after light onset (Fig. 3*C*). Changes in cathepsin D activity occurred specifically in the RPE/choroid because we did not detect differences in cathepsin D activity with time of day in neural retina extracts from either $^{RPE}CAV1^{+/+}$ or $^{RPE}CAV1^{-/-}$ mice (Fig. 3*C*). In addition, we tested the activity profile of another lysosomal enzyme, β-*N*-acetylglucosaminidase, which is essential for deglycosylation of phagocytosed POS-opsin (37,

38). The enzyme activity profiles of β-*N*-acetyl-glucosaminidase 0.5 and 8 h post-light onset mirrored that of cathepsin D for $^{RPE}CAV1^{+/+}$ and $^{RPE}CAV1^{-/-}$ RPE/choroid tissues fractions (Fig. 3*D*). Similar to cathepsin D, there was no change in enzymatic activity in neural retina fractions (Fig. 3*D*). Activities of both enzymes were ~10-fold lower in neural retina fractions than the respective activities in RPE/choroid fractions (Fig. 3, *C* and *D*). Despite high enzyme activity in $^{RPE}CAV1^{-/-}$ RPE, undigested POS phagosomes remained at the 8-h time point tested. We conclude that the 8-h time point represents early or just prior to onset of phagosome digestion, which is accomplished by $^{RPE}CAV1^{-/-}$ RPE in time for the next POS challenge (Fig. 2*B*, *−1 h time point*). Next, we tested whether recruitment of cathepsin D to POS-opsin phagosomes may require caveolin-1 by double-labeling phagosomes with opsin N terminus and cathepsin D antibodies. In this experiment, we established the fraction of cathepsin D-positive phagosomes in each sample, a value that is independent of absolute phagosome numbers, which vary among the samples, as shown in Fig. 2. We found that the percentage of opsin/cathepsin D double-positive phagosomes was similar for $^{RPE}CAV1^{+/+}$ and $^{RPE}CAV1^{-/-}$ RPE at both early and late time points. This suggests that cathepsin D recruitment was not affected by caveolin-1 deficiency (Fig. 3, *E* and *F*).

Caveolin-1 Localizes to Phagolysosomes in RPE Cells—To directly test whether caveolin-1 contributes to POS digestion, we examined the role of caveolin-1 in phagocytic RPE cells in culture. The rat RPE-derived RPE-J cell line possesses and employs the same phagocytic pathway via αvβ5 integrin and Mer tyrosine kinase receptors as RPE *in situ*, and it has been used extensively for POS uptake studies previously (39–42). Here we used a two-phase phagocytosis assay to synchronize POS engulfment and processing (28), followed by triple-labeling of opsin, LysoTracker (to specifically label acidified phagolysosomes), and caveolin-1. We challenged polarized RPE cells with POS particles for 1 h at 20 °C (pulse), a temperature that allows normal POS binding by the RPE-J cell line (via αvβ5 integrin) but does not allow internalization (43). Caveolin-1 did not colocalize with bound POS immediately after the pulse (Fig. 4*A1*). Caveolin-1 labeling was abundant in the cell cytoplasm, where, as expected, there were no engulfed POS (Fig. 4*A2*). After 2 h of further incubation at a permissive temperature (chase), we found that some (but not all) engulfed POS were acidified, but these did not co-stain with caveolin-1 antibody (Fig. 4*B*). After 6 h of chase, most POS-opsin-positive phagosomes were acidified, and caveolin-1, in part, co-localized with these phagolysosomes (Fig. 4*C*). Quantification of LysoTracker and caveolin-1 labeling of opsin-positive phagosomes confirmed that caveolin-1, but not LysoTracker, was largely absent from early engulfed phagosomes (Fig. 4*D*). In contrast, cathepsin D and the lysosomal organelle protein LAMP-1 localized to early as well as late engulfed POS (Fig. 4, *E–H*). Therefore, caveolin-1 resides only on engulfed phagosomes at a specific stage but not on early internalized phagosomes. Notably, this suggests that engulfed phagosomes acquire caveolin-1 decoration *de novo* rather than carrying it with them from the internalized plasma membrane.

Increasing or Decreasing Caveolin-1 in RPE Cells in Culture Is Sufficient to Accelerate or Slow Down Phagolysosomal Digestion, Respectively—To confirm our *in vivo* results and further specify the direct role of caveolin-1 in the phagocytic process, we next tested POS uptake and digestion by RPE cells in culture after manipulating caveolin-1 expression. First, we transiently overexpressed either WT or a mutant form of caveolin-1 containing F92A and V94A point mutations in the scaffolding domain or β-galactosidase as a control by recombinant adenovirus transduction (Fig. 5*A*). Mut-caveolin-1 is defective in plasma membrane localization and prevents caveola internalization of ligands but retains functionality at cytoplasmic sites (29, 44, 45). Exogenous WT- and mut-caveolin-1 were both tagged with the myc epitope and expressed at similar levels, increasing total caveolin-1 protein levels to ~2.4-fold (Fig. 5*B*). In synchronized POS phagocytosis assays, we observed similar initial POS binding immediately regardless of expression of WT- or mut-caveolin-1 (Fig. 5, *C* and *D*, *lanes* and *columns*, respectively, *0 h chase*). This confirms and extends our *in vivo* phagocytosis quantification, indicating that caveolin-1 is not involved in POS binding. However, quantification of POS-opsin after different periods of chase showed that cells overexpressing either WT- or mut-caveolin-1 eliminated engulfed POS significantly faster than control cells, specifically later in the chase (Fig. 5, *C* and *D*, *lanes* and *columns*, respectively, *5* and *8 h chase*). Differences between caveolin-1-overexpressing and control cells were most pronounced at the late 8-h time point, indicating that increasing levels of either WT or mutant caveolin-1 is sufficient to accelerate phagosome digestion. These results suggest that the caveolin scaffolding domain is not involved in the ability of caveolin-1 to modulate phagocytosis. Next we examined the effect of silencing caveolin-1 expression on RPE phagocytosis. Infection of RPE cells with a caveolin-1-silencing lentivirus reduced caveolin-1 protein levels by ~50% compared with control cells that received a non-targeting lentivirus (Fig. 5, *E* and *F*). Reducing the levels of caveolin-1 did not alter POS binding (Fig. 5, *G* and *H*, *0 h lanes* and *columns*, respectively) but caused persistent POS-opsin in cells at later times of chase (Fig. 5, *G* and *H*, *5* and *8 h lanes* and *columns*, respectively). We conclude that decreasing the levels of caveolin-1 slows down phagosome digestion. Together, our *in vivo* and cell culture results are in complete agreement and indicate that caveolin-1 contributes to the digestion phase of phagocytosis. Moreover, its contribution does not require an intact scaffolding domain that promotes caveolin-1 function at the cell surface.

Silencing Caveolin-1 Is Sufficient to Alter Cathepsin D and β-N-acetylglucosaminidase Activity and Alkalinize Lysosomal pH in Resting RPE Cells and to Preclude Maturation and Activation of Cathepsin D during POS Phagocytosis—To determine how caveolin-1 affects phagolysosomal digestion, we next compared the lysosomal characteristics of caveolin-1-silenced and -competent RPE cells in culture. As observed for RPE *in vivo*, we found that decreasing caveolin-1 in cultured RPE caused moderate but significant decreases in the activity of the phagolysosomal enzymes cathepsin D and β-*N*-acetylglucosaminidase (Fig. 6, *A* and *B*). Moreover, lysosomes in caveolin-1-silenced cells were significantly less acidic than lysosomes in control

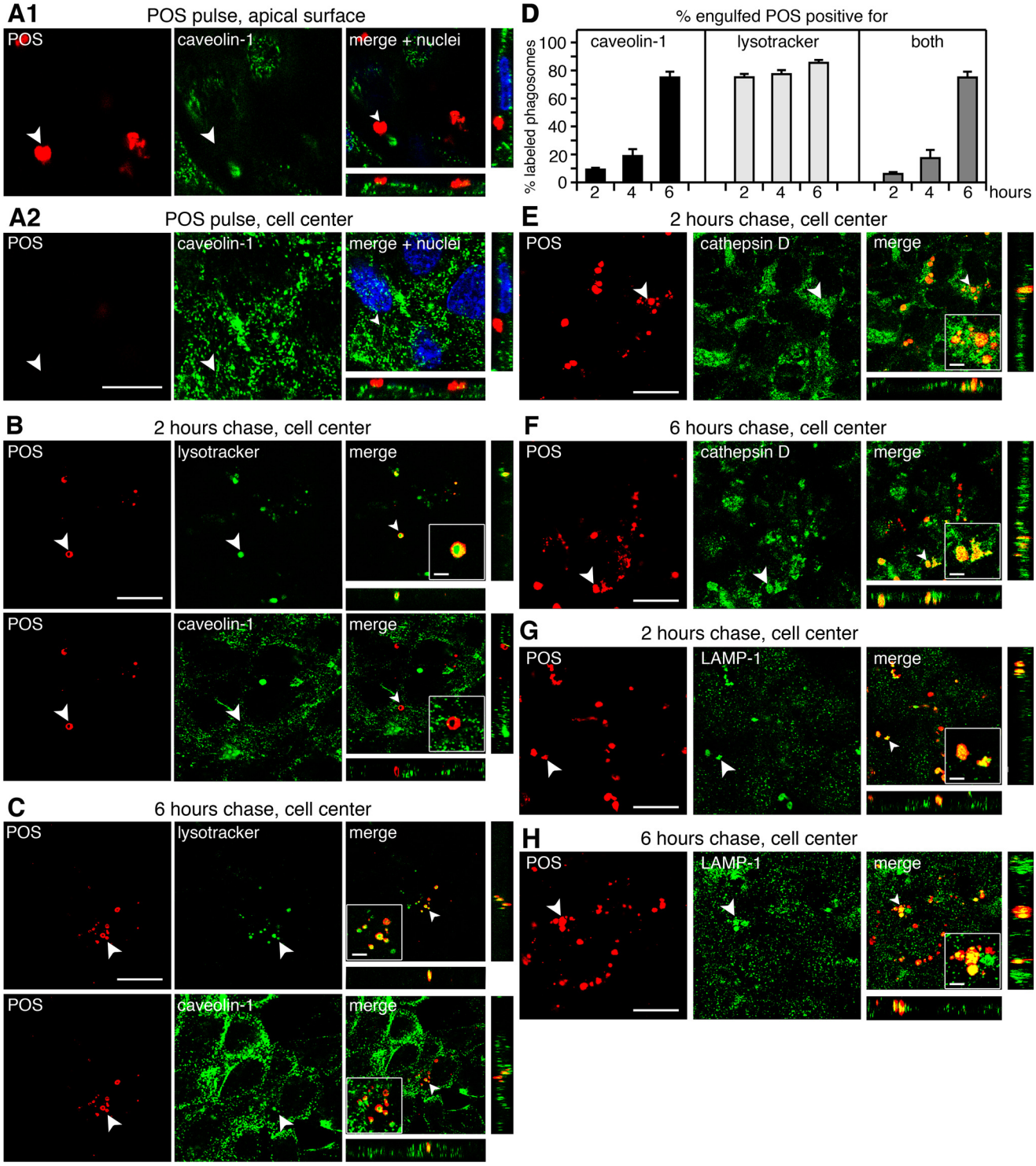

FIGURE 4. **Endogenous caveolin-1 localizes to POS phagosomes in RPE cells in culture during the digestion phase.** Polarized RPE-J cells were challenged at 20 °C with POS for 1 h (pulse) before washing and continued incubation at a permissive temperature for 2 or 6 h (chase, as indicated). All fields show representative single *x-y* planes from image stacks of labels, as indicated, of at least three independent experimental repeats. *Insets* show magnified areas. *Arrowheads* point out example POS. For merged images, *x-z* views are also provided. *Scale bars* = 10 μm. *Scale bars for magnified insets* = 2 μm. *A*, bound POS localize to the apical surface (*A1*) but not to the cell interior (*A2*) immediately after pulse. Caveolin localizes to the surface and cytoplasm but does not colocalize with POS (*merge*). The *merged panel* also shows nuclei (*blue*). *B*, after 2 h of chase, engulfed POS co-localize with LysoTracker (*green*, *top panels*) but not with caveolin-1 (*green*, *bottom panels*). Both LysoTracker and caveolin-1 are shown in *green* for the ease of showing co-localization. They were imaged in red and green channels, respectively, whereas POS were imaged in far-red. *C*, after 6 h of chase, POS (*red*) co-localize with both LysoTracker (*green*, *top panels*) and with caveolin-1 (*green*, *bottom panels*). Imaging was as in *B*. *D*, quantification of engulfed POS colocalizing with caveolin-1 (*black columns*), LysoTracker (*light gray columns*), or both (*dark gray columns*) after 2, 4, and 6 h of chase. *Error bars* show mean ± S.E. ($n = 3$). *E* and *F*, engulfed POS (*red*) co-localize with cathepsin D (*green*) after 2 h (*E*) and 6 h of chase (*F*). *G* and *H*, engulfed POS (*red*) co-localize with Lamp-1 (*green*) after 2 h (*G*) and 6 h of chase (*H*).

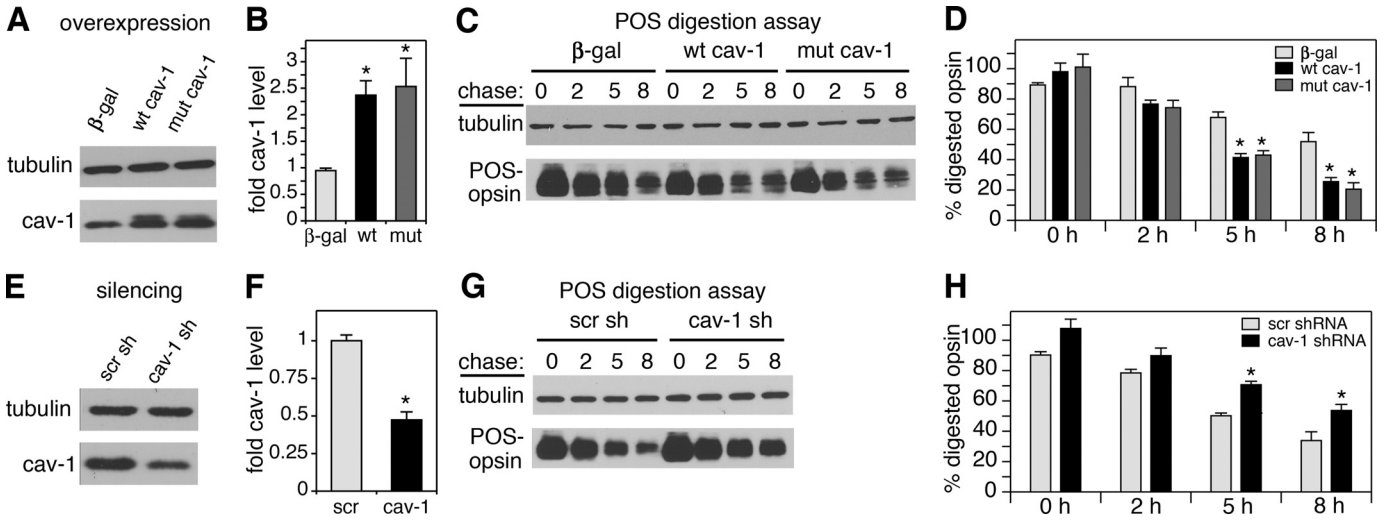

FIGURE 5. **Increasing or decreasing caveolin-1 in RPE cells in culture is sufficient to accelerate or slow down phagolysosomal digestion, respectively.** *A–D*, confluent RPE-J cells were infected with recombinant adenovirus encoding β-gal as a control, WT cav-1, or mutant caveolin-1 that does not reach the plasma membrane before phagocytosis assay and/or lysis. *A*, representative immunoblot showing transient overexpression of either form of caveolin-1 and tubulin reblot of the same membrane as a loading control. *B*, comparison of caveolin-1 protein levels relative to tubulin levels. Relative caveolin-1 levels in cells expressing β-galactosidase (*light gray columns*) were set as 1. *Black columns*, cells expressing WT caveolin-1; *dark gray columns*, cells expressing mutant caveolin-1. *Error bars* show mean ± S.E. ($n = 4$ independent experiments with duplicates each). *C*, representative immunoblot showing POS-opsin content of cells infected as indicated before challenge with POS for 1 h and chase for 0–8 h as indicated. A tubulin reblot of the same membrane is also shown as a loading control. *D*, quantification of phagolysosomal digestion of POS-opsin by RPE cells in culture in phagocytosis experiments as in *C*. In all samples, relative levels of POS-opsin to tubulin were first calculated and then compared with relative POS-opsin levels in control cells expressing β-galactosidase lysed after 0 h of chase. Note that all cells tested possess the same relative POS-opsin levels after 0 h of chase, confirming that increasing caveolin-1 does not affect POS binding. Column colors are as in *B* and as indicated in the legend. *Error bars* show mean ± S.E. ($n = 4$ independent experiments with duplicates each). *E–H*, RPE-J cells were infected with a lentivirus encoding scrambled (*scr*), non-silencing shRNA as control or shRNA specific to caveolin-1 (*cav-1 sh*) before selection of stable transduced populations and phagocytosis experiments and/or lysis. *E*, representative immunoblot showing decreased caveolin-1 expression in cells with silenced caveolin-1 and tubulin reblot of the same membrane as a loading control. *F*, comparison of caveolin-1 protein levels relative to tubulin levels. Relative caveolin-1 levels in control cells transduced with a lentivirus encoding scrambled RNA (*light gray columns*) were set as 1. *Black columns* show caveolin-1 in cells in which caveolin-1 was silenced. *Error bars* show mean ± S.E. ($n = 4$ independent experiments with duplicates each). *G*, representative immunoblot showing POS-opsin content of cells selected to express silencing RNA, as indicated, before challenge with POS for 1 h and chase for 0–8 h, as indicated. A tubulin reblot of the same membrane is also shown as a loading control. *H*, quantification of phagolysosomal digestion of POS-opsin by RPE cells in culture in phagocytosis experiments as in *G*. In all samples, relative levels of POS-opsin to tubulin were first calculated and then compared with relative POS-opsin levels in control cells lysed after 0 h of chase. Note that both cell populations tested possess the same relative POS-opsin levels after 0 h of chase, confirming that decreasing caveolin-1 does not affect POS binding. Column colors are as in *F* and as indicated in the legend. *Error bars* show mean ± S.E. ($n = 4$ independent experiments with duplicates each). Significant differences between test and control samples in each experiment are indicated as *, $p < 0.05$ by ANOVA (*B*, *D*, and *H*) or Student's *t* test (*F*). Values presented in all unmarked columns do not significantly differ from the control.

cells (Fig. 6*C*). In contrast, lysosome numbers, vesicle area, and lysosomal subcellular distribution were not affected by caveolin-1 silencing (Fig. 6, *D–F*). We conclude that decreasing caveolin-1 is sufficient to impair lysosomal activity in resting RPE cells without phagocytic load. We also found that POS challenge and degradation did not change lysosomal pH in either control or caveolin-1-silenced cells, which remained different throughout the process (Fig. 6*G*). However, cathepsin D proteolytic processing to the mature form and a rise in cathepsin D enzymatic activity occurred in control RPE cells but not in RPE cells with reduced levels of caveolin-1 (Fig. 6, *H–J*). These data show that RPE cells up-regulate cathepsin D activity in response to POS phagolysosomal load using a mechanism that depends on caveolin-1. They suggest that the activity increase after light onset we observed in $^{RPE}CAV1^{+/+}$ *in situ* is a direct response by RPE cells to POS uptake rather than an entrained diurnal mechanism.

Silencing Caveolin-1 Affects the Constitutive Lysosomal Degradation of Transferrin Receptors without Affecting Steady-state Transferrin Receptor Levels—Finally, we tested whether a lysosomal degradation process unrelated to POS phagocytosis was also affected by the moderate changes in lysosomal function observed in caveolin-1-silenced RPE cells in culture. We chose to study the lysosomal turnover of transferrin receptors, a recently described slow, constitutive degradation pathway (46). First, we established the time course of lysosomal degradation by RPE cells with normal levels of caveolin-1 (Fig. 7, *A* and *B*). Upon treatment with cycloheximide to halt protein synthesis, cells showed normal levels of transferrin receptor for 1 and 2 h but significantly reduced levels after 3 and 5 h (Fig. 7*B*). At the 3-h (but not the 5-h) time point, the levels of caveolin-1 were normal, indicating that the treatment was not inducing dramatic cell damage (Fig. 7*A*). Therefore, in a second experiment, we chose a 3-h treatment time to compare the effects of cycloheximide treatment on transferrin receptor levels in control cells and cells with reduced levels of caveolin-1 (Fig. 7, *C* and *D*). We found that cycloheximide treatment did not reduce transferrin receptor levels in caveolin-1-silenced cells like in control cells (Fig. 7*D*). Decreasing lysosomal activity by treatment with bafilomycin A eliminated the effect of cycloheximide on control cells, confirming the lysosomal dependence of transferrin receptor turnover. Bafilomycin A alone had no effect on receptor levels, implying that cells may adjust receptor synthesis to maintain normal receptor levels over the 3-h time period.

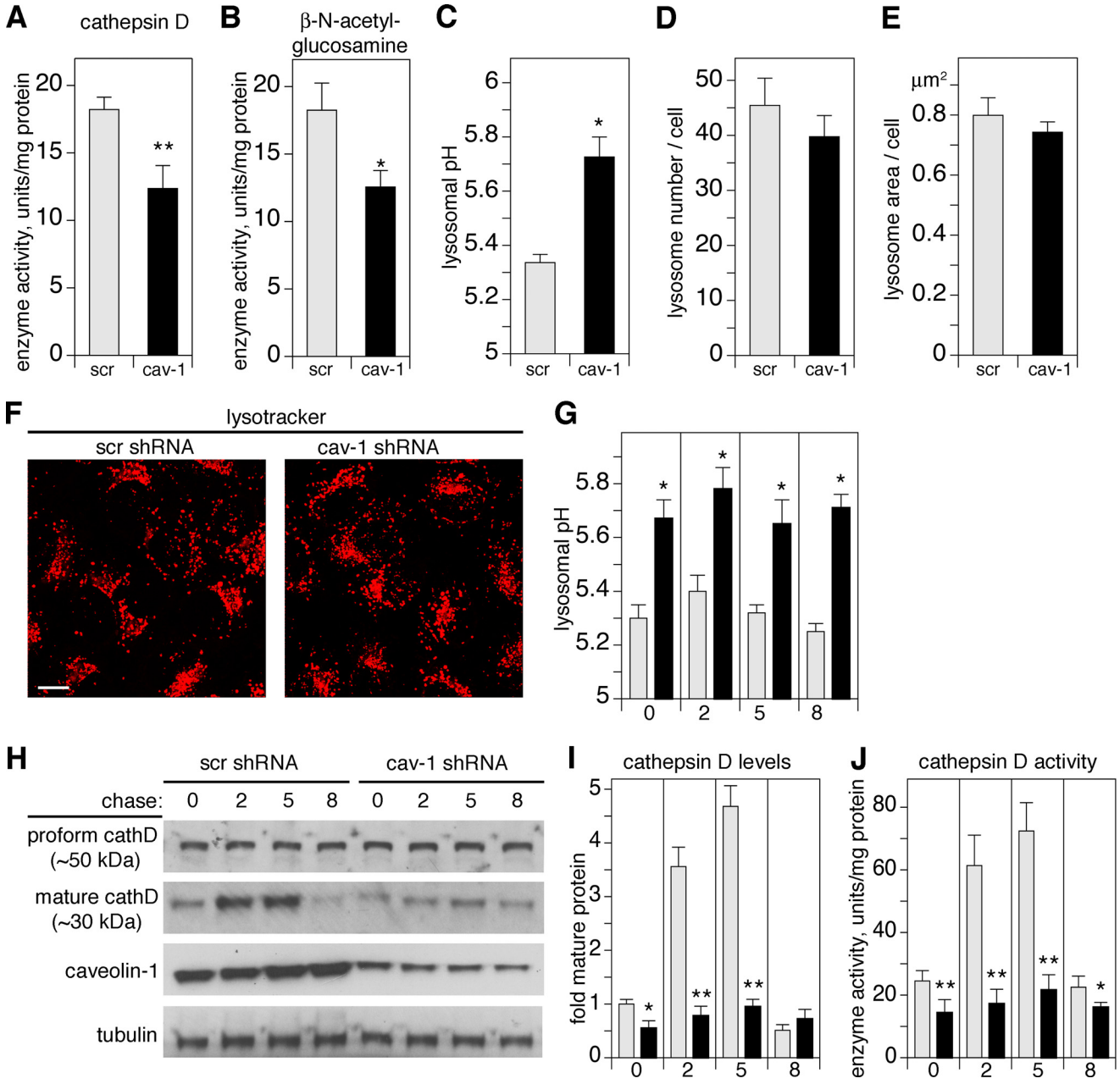

FIGURE 6. **Decreasing caveolin-1 reduces the activity of lysosomal enzymes and pH values without altering lysosomal morphology or abundance in resting cells in culture and reduces the stimulation of cathepsin D processing and activity during POS phagocytosis.** Stably selected populations of RPE-J cells expressing scrambled, non-silencing shRNA as a control (*scr*, *gray columns*) or shRNA specific to caveolin-1 (*black columns*) were grown to post-confluence before analysis of lysosomal parameters in resting cells or cells following POS challenge and chase. *A–F*, lysosomal characteristics of resting cells. *A*, quantification of cathepsin D enzymatic activity. *B*, quantification of *β-N*-acetyl-glucosamine enzymatic activity. *C*, comparison of lysosomal pH values. *D*, comparison of the number of lysosomes per cell. *E*, comparison of the area of individual lysosomal vesicles. *F*, representative LysoTracker live staining images. Single *x-y* confocal planes are shown. Images were acquired using identical imaging parameters and processed identically. *Scale bar* = 10 μm. *G–J*, lysosomal characteristics of cells in synchronized pulse-chase POS phagocytosis assays. *G*, quantification of lysosomal pH values after POS binding pulse (0 h) and chase for 2, 5, or 8 h, as indicated. ANOVA did not reveal differences with time in either cell type but showed differences between control and cav-1-silenced cells at all time points. *H*, immunoblot detection of the immature preform and the cleaved, mature form of cathepsin D (*cathD*) during POS phagocytosis. Immunoblot detection of caveolin-1 confirmed its reduction in silenced cells, and tubulin served as a loading control. A representative blot membrane of three independent experiments is shown that was incubated sequentially with all three probes. *I*, relative change of the mature form of cathepsin D during POS phagocytosis. ANOVA showed significant differences between control and cav-1-silenced cells at the same time point. -Fold mature protein is presented relative to tubulin levels in each sample. Levels in control cells after POS pulse (*0 h*) are set as 1. *J*, quantification of cathepsin D enzymatic activity in cells lysed after POS binding pulse (0 h) or 2, 5, or 8 h after chase as indicated. Significant differences between cell types at the same time point were established by ANOVA. All experiments were performed at least three times independently with duplicates or triplicates. All *error bars* show mean ± S.E. Significant differences of cells with silenced caveolin-1 compared with cells expressing control silencing shRNA were established by Student's *t* test or, if stated, by ANOVA followed by Tukey's post hoc test. *, $p < 0.05$; **, $p < 0.01$.

This agrees well with the finding that solvent-treated cells with reduced levels of caveolin-1 maintain normal transferrin receptor levels (Fig. 7*D*, *n.s.*). These data suggest that RPE cells can compensate for the moderate lysosomal defect caused by reducing caveolin-1 expression to maintain normal transferrin receptor levels.

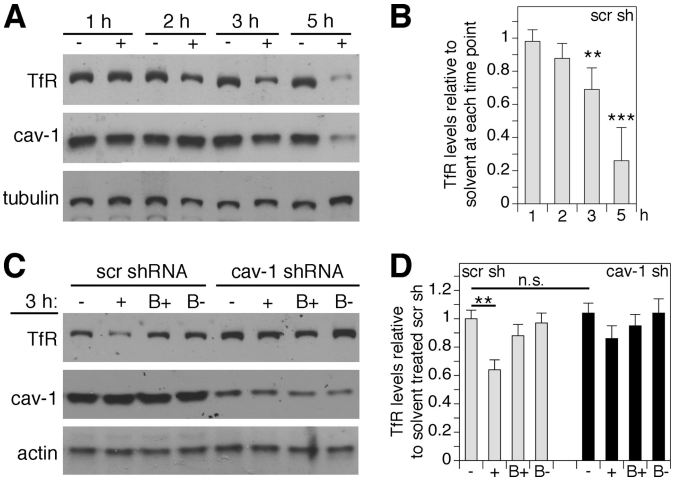

FIGURE 7. **Decreasing caveolin-1 in RPE cells in culture reduces the turnover rate of transferrin receptor without an effect on steady-state levels.** Stably selected populations of RPE-J cells expressing scrambled, non-silencing shRNA as control (*scr sh*, *gray columns*) or shRNA specific to caveolin-1 (*cav-1 sh*, *black columns*) were grown to post-confluence before treatment with cycloheximide (+), with cycloheximide plus bafilomycin A (*B*+), with solvent (−), or with solvent plus bafilomycin A (*B*−) before lysis and immunoblotting analysis of transferrin receptor (*TfR*), caveolin-1, tubulin, or actin as indicated. Blots show representative membranes of three independent experiments probed sequentially for transferrin receptor, caveolin-1, and a loading control. All *error bars* show mean ± S.D. *A*, control cells were lysed after 1–5 h of treatment with (+) or without (−) cycloheximide. *B*, quantification of transferrin receptor protein levels in cycloheximide-treated cells relative to untreated cells. Cells were treated as in *A*. Transferrin receptor levels were reduced significantly at 3 and 5 h of treatment, as established by Student's *t* test. **, $p < 0.01$; **, $p < 0.001$. *C*, comparison of transferrin receptor, caveolin-1, and actin protein content in cells with control or reduced caveolin-1 levels after 3-h treatment as indicated and described above. *D*, quantification of transferrin receptor protein levels in samples obtained as in *C*. All *error bars* show relative levels compared with levels in control cells treated with solvent, which was set as 1. Comparing treatment effects with solvent for each cell population, ANOVA shows a significant reduction only for cycloheximide treatment of control cells (**, $p < 0.01$; *n.s.*, not significant). All other treatments did not differ from solvent treatment. Cycloheximide treatment of control cells also differed significantly from bafilomycin A alone and cycloheximide plus bafilomycin A (not indicated in the figure). Comparing cell populations, transferrin receptor levels did not differ between solvent-treated control and caveolin-1-silenced cells (*n.s.*), indicating that cells with reduced levels of caveolin-1 maintain normal steady-state transferrin receptor levels.

Discussion

Caveolin-1 is a ubiquitous protein that contributes to numerous cell and tissue functions. Global caveolin-$1^{-/-}$ mice exhibit decreased rod-mediated function. However, caveolin-$1^{-/-}$ rod photoreceptors retain the capacity to detect photons and stimulate phototransduction in principle (17). Here we show significant impairment in rod photoreceptor function *in vivo* in mice with normal caveolin-1 expression in rods and other neuroretinal cells but engineered to lack caveolin-1 specifically in the neighboring RPE. To our knowledge, our study is the first to demonstrate a non-cell autonomous effect of tissue-specific knockout of caveolin-1 and to illustrate the utility of such animal models. Although our data clarify that RPE caveolin-1 is essential for rod function, future studies quantifying vision of mice lacking caveolin-1 only in mature rods will need to examine whether or not rod caveolin-1 is also important for rod phototransduction.

Probing putative roles for caveolin-1 in support functions of the RPE for rods, we scrutinized diurnal outer segment clearance because it is critical for retinal homeostasis and relies on dynamics in membrane properties and signaling caveolin-1 is known to be able to facilitate (19, 47, 48). Our *in vivo* and cell culture experiments agree that caveolin-1 regulates the efficiency of phagolysosomal digestion by RPE cells. We detected caveolin-1 on phagolysosomes and found that expression of mutant caveolin-1 that does not reach the plasma membrane is effective in accelerating digestion. We conclude that a cytoplasmic pool rather than a plasma membrane pool of caveolin-1 is relevant to phagolysosomal digestion. To our knowledge, these are the first data implicating caveolin-1 in digestion in any phagocytic mechanism.

We found that the initial steps of clearance phagocytosis, recognition/binding and engulfment, are independent of caveolin-1 both in RPE *in vivo* and in culture. Earlier work has shown a reduction in phagocytosis of apoptotic cells or *Escherichia coli* by about 20% in thioglycollate-elicited macrophages from caveolin-$1^{-/-}$ mice compared with macrophages from caveolin-$1^{+/+}$ mice (49). This study did not probe distinct steps of phagocytosis but reported total particle uptake after short-term particle incubation. The effects seen were therefore likely due to altered particle binding or engulfment. Therefore, although both RPE and elicited macrophages are avid phagocytes, only macrophages seem to employ caveolin-1 in the uptake phase of phagocytosis. These cell types also employ different phagocytic receptors. RPE cells like non-elicited macrophages and immature dendritic cells utilize a pathway dependent on $\alpha v\beta 5$ integrin whereas elicited macrophages do not. We have shown previously that the particle recognition mechanism used by RPE cells requires activation of the particle recognition/binding receptor $\alpha v\beta 5$ integrin by interaction with the tetraspanin CD81 (50). We speculate that tetraspanin and caveolin-1 may play similar roles in particle recognition/binding/engulfment in RPE cells and macrophages, respectively.

Mechanistically, our experiments show a role for caveolin-1 in regulating lysosomal function by promoting lysosomal acidification. Reduced lysosomal enzyme activities and more alkaline lysosomal pH even in resting RPE cells suggests that caveolin-1 does not only act on the lysosomal system in actively phagocytic cells. Indeed, we show that cells manipulated to lack protein synthesis do not degrade transferrin receptors, a constitutive lysosomal turnover process. However, unmanipulated cells maintain normal transferrin receptor levels. We conclude that RPE cells with reduced levels of caveolin-1 are able to maintain normal degradation processes despite moderate impairment of lysosomal organelles. In contrast, the high and acute load of protein and lipids in POS phagolysosomes may be especially sensitive to moderate changes in lysosomal function and pH and, therefore, allowed us to detect changes in the rate of digestion both in culture and *in vivo*. In our RPE cell culture systems, even a reduction by 50% of caveolin-1 was sufficient to significantly delay phagosome digestion. RPE phagosomes mature in two steps: initial weak to moderate acidification and a stronger secondary acidification that is required for digestion. Step 1 occurs in a kiss-and-run type mechanism that transfers soluble enzymes like cathepsin D, whereas step 2 requires *bona fide* membrane fusion of lysosomes with phagosomes (6, 7). Our data show that caveolin-1 is not involved in recruitment of

cathepsin D, which is acquired in step 1 by early phagosomes. Similar decreases in both cathepsin D and β-*N*-acetylglucosaminidase activity by lack or reduction of caveolin-1 *in vivo* or in cell culture further suggest that enzyme activity is not specifically altered. Phagosome maturation in step 2 is accelerated by caveolin-1, and decreasing levels of caveolin-1 even by only 50% increases lysosomal pH values. Changes in cathepsin D maturation and activation in response to a single burst of POS phagocytosis by RPE cells in culture show that RPE cells respond directly to uptake of POS into early lysosomal compartments with enzyme activity regulation compared with being entrained to a diurnal cycle of enzyme activity. Together, although the changes in lysosomal activity caused by loss of caveolin-1 in the RPE are modest, they have significant physiological consequences because of the very high and life-long phagocytic burden of post-mitotic RPE cells.

Our results contribute novel mechanistic insights to the growing body of evidence regarding the importance of intracellular caveolin-1 in endo/lysosomal organelle traffic and degradation. Fibroblasts and breast cancer cells in culture lacking caveolin-1 increase autophagy markers and LysoTracker-positive compartments in a response to increased oxidative stress (51, 52). Notably, non-canonical autophagy shares components with clearance phagocytosis pathways (53, 54). Recent studies have demonstrated the importance of caveolin-1 in multifunctional endosomal and lysosomal compartments (21, 55). Our results extend these observations, showing that phagosomes are regulated by caveolin-1 as well. Moreover, we provide the first direct evidence that caveolin-1 is of physiological significance for intracellular degradative pathways *in vivo*.

Author Contributions—S. S. designed experiments, performed experiments, analyzed results, and wrote the paper. T. C. and X. G. performed experiments and analyzed results. G. C. and T. C. T. provided critical models and tools. M. H. E. designed experiments, performed experiments, and interpreted data. S. C. F. designed experiments, performed experiments, interpreted data, and wrote the paper. All authors reviewed the results and approved the final version of the manuscript.

Acknowledgments—We thank Dr. Patricio Meneses (Fordham University) for caveolin-1 expression plasmids and Dr. Paul Hargrave for providing B6-30 hybridoma cells. We also thank Dr. Yun Le (University of Oklahoma Health Sciences Center) for inducible RPE-cre mice.

References

1. Strauss, O. (2005) The retinal pigment epithelium in visual function. *Physiol. Rev.* **85,** 845–881
2. Young, R. W. (1967) The renewal of photoreceptor cell outer segments. *J. Cell Biol.* **33,** 61–72
3. Young, R. W., and Bok, D. (1969) Participation of the retinal pigment epithelium in the rod outer segment renewal process. *J. Cell Biol.* **42,** 392–403
4. LaVail, M. M. (1976) Rod outer segment disk shedding in rat retina: relationship to cyclic lighting. *Science* **194,** 1071–1074
5. Sethna, S., and Finnemann, S. C. (2013) Analysis of photoreceptor rod outer segment phagocytosis by RPE cells *in situ*. *Methods Mol. Biol.* **935,** 245–254
6. Bosch, E., Horwitz, J., and Bok, D. (1993) Phagocytosis of outer segments by retinal pigment epithelium: phagosome-lysosome interaction. *J. Histochem. Cytochem.* **41,** 253–263
7. Deguchi, J., Yamamoto, A., Yoshimori, T., Sugasawa, K., Moriyama, Y., Futai, M., Suzuki, T., Kato, K., Uyama, M., and Tashiro, Y. (1994) Acidification of phagosomes and degradation of rod outer segments in rat retinal pigment epithelium. *Invest. Ophthalmol. Vis. Sci.* **35,** 568–579
8. Nandrot, E. F., Kim, Y., Brodie, S. E., Huang, X., Sheppard, D., and Finnemann, S. C. (2004) Loss of synchronized retinal phagocytosis and age-related blindness in mice lacking αvβ5 integrin. *J. Exp. Med.* **200,** 1539–1545
9. Damek-Poprawa, M., Diemer, T., Lopes, V. S., Lillo, C., Harper, D. C., Marks, M. S., Wu, Y., Sparrow, J. R., Rachel, R. A., Williams, D. S., and Boesze-Battaglia, K. (2009) Melanoregulin (MREG) modulates lysosome function in pigment epithelial cells. *J. Biol. Chem.* **284,** 10877–10889
10. Rakoczy, P. E., Zhang, D., Robertson, T., Barnett, N. L., Papadimitriou, J., Constable, I. J., and Lai, C. M. (2002) Progressive age-related changes similar to age-related macular degeneration in a transgenic mouse model. *Am. J. Pathol.* **161,** 1515–1524
11. Sparrow, J. R., Hicks, D., and Hamel, C. P. (2010) The retinal pigment epithelium in health and disease. *Curr. Mol. Med.* **10,** 802–823
12. Valapala, M., Wilson, C., Hose, S., Bhutto, I. A., Grebe, R., Dong, A., Greenbaum, S., Gu, L., Sengupta, S., Cano, M., Hackett, S., Xu, G., Lutty, G. A., Dong, L., Sergeev, Y., Handa, J. T., Campochiaro, P., Wawrousek, E., Zigler, J. S., Jr., and Sinha, D. (2014) Lysosomal-mediated waste clearance in retinal pigment epithelial cells is regulated by CRYBA1/βA3/A1-crystallin via V-ATPase-MTORC1 signaling. *Autophagy* **10,** 480–496
13. Mora, R. C., Bonilha, V. L., Shin, B. C., Hu, J., Cohen-Gould, L., Bok, D., and Rodriguez-Boulan, E. (2006) Bipolar assembly of caveolae in retinal pigment epithelium. *Am. J. Physiol. Cell Physiol.* **290,** C832–C843
14. Gu, X., Reagan, A., Yen, A., Bhatti, F., Cohen, A. W., and Elliott, M. H. (2014) Spatial and temporal localization of caveolin-1 protein in the developing retina. *Adv. Exp. Med. Biol.* **801,** 15–21
15. Gu, X., Fliesler, S. J., Zhao, Y. Y., Stallcup, W. B., Cohen, A. W., and Elliott, M. H. (2014) Loss of caveolin-1 causes blood-retinal barrier breakdown, venous enlargement, and mural cell alteration. *Am. J. Pathol.* **184,** 541–555
16. Reagan, A., Gu, X., Hauck, S. M., Ash, J. D., Cao, G., Thompson, T. C., and Elliott, M. H. (2016) Retinal caveolin-1 modulates neuroprotective signaling. *Adv. Exp. Med. Biol.* **854,** 411–418
17. Li, X., McClellan, M. E., Tanito, M., Garteiser, P., Towner, R., Bissig, D., Berkowitz, B. A., Fliesler, S. J., Woodruff, M. L., Fain, G. L., Birch, D. G., Khan, M. S., Ash, J. D., and Elliott, M. H. (2012) Loss of caveolin-1 impairs retinal function due to disturbance of subretinal microenvironment. *J. Biol. Chem.* **287,** 16424–16434
18. Boscher, C., and Nabi, I. R. (2012) Caveolin-1: role in cell signaling. *Adv. Exp. Med. Biol.* **729,** 29–50
19. Fridolfsson, H. N., Roth, D. M., Insel, P. A., and Patel, H. H. (2014) Regulation of intracellular signaling and function by caveolin. *FASEB J.* **28,** 3823–3831
20. Kurzchalia, T. V., Dupree, P., and Monier, S. (1994) VIP21-Caveolin, a protein of the trans-Golgi network and caveolae. *FEBS Lett.* **346,** 88–91
21. He, K., Yan, X., Li, N., Dang, S., Xu, L., Zhao, B., Li, Z., Lv, Z., Fang, X., Zhang, Y., and Chen, Y. G. (2015) Internalization of the TGF-β type I receptor into caveolin-1 and EEA1 double-positive early endosomes. *Cell Res.* **25,** 738–752
22. Adamus, G., Zam, Z. S., Arendt, A., Palczewski, K., McDowell, J. H., and Hargrave, P. A. (1991) Anti-rhodopsin monoclonal antibodies of defined specificity: characterization and application. *Vision Res.* **31,** 17–31
23. Chucair-Elliott, A. J., Elliott, M. H., Wang, J., Moiseyev, G. P., Ma, J. X., Politi, L. E., Rotstein, N. P., Akira, S., Uematsu, S., and Ash, J. D. (2012) Leukemia inhibitory factor coordinates the down-regulation of the visual cycle in the retina and retinal-pigmented epithelium. *J. Biol. Chem.* **287,** 24092–24102
24. Le, Y. Z., Zheng, W., Rao, P. C., Zheng, L., Anderson, R. E., Esumi, N., Zack, D. J., and Zhu, M. (2008) Inducible expression of cre recombinase in the retinal pigmented epithelium. *Invest. Ophthalmol. Vis. Sci.* **49,** 1248–1253
25. Cao, G., Yang, G., Timme, T. L., Saika, T., Truong, L. D., Satoh, T., Goltsov, A., Park, S. H., Men, T., Kusaka, N., Tian, W., Ren, C., Wang, H., Kadmon, D., Cai, W. W., Chinault, A. C., Boone, T. B., Bradley, A., and Thompson,

T. C. (2003) Disruption of the caveolin-1 gene impairs renal calcium reabsorption and leads to hypercalciuria and urolithiasis. *Am. J. Pathol.* **162,** 1241–1248
26. Mandal, M. N., Moiseyev, G. P., Elliott, M. H., Kasus-Jacobi, A., Li, X., Chen, H., Zheng, L., Nikolaeva, O., Floyd, R. A., Ma, J. X., and Anderson, R. E. (2011) α-phenyl-*N*-tert-butylnitrone (PBN) prevents light-induced degeneration of the retina by inhibiting RPE65 protein isomerohydrolase activity. *J. Biol. Chem.* **286,** 32491–32501
27. Finnemann, S. C., and Rodriguez-Boulan, E. (1999) Macrophage and retinal pigment epithelium phagocytosis: apoptotic cells and photoreceptors compete for αvβ3 and αvβ5 integrins, and protein kinase C regulates αvβ5 binding and cytoskeletal linkage. *J. Exp. Med.* **190,** 861–874
28. Mao, Y., and Finnemann, S. C. (2013) Analysis of photoreceptor outer segment phagocytosis by RPE cells in culture. *Methods Mol. Biol.* **935,** 285–295
29. Nystrom, F. H., Chen, H., Cong, L. N., Li, Y., and Quon, M. J. (1999) Caveolin-1 interacts with the insulin receptor and can differentially modulate insulin signaling in transfected Cos-7 cells and rat adipose cells. *Mol. Endocrinol.* **13,** 2013–2024
30. Parinot, C., Rieu, Q., Chatagnon, J., Finnemann, S. C., and Nandrot, E. F. (2014) Large-scale purification of porcine or bovine photoreceptor outer segments for phagocytosis assays on retinal pigment epithelial cells. *J. Vis. Exp.* **12,** 10.3791/52100
31. Guha, S., Coffey, E. E., Lu, W., Lim, J. C., Beckel, J. M., Laties, A. M., Boesze-Battaglia, K., and Mitchell, C. H. (2014) Approaches for detecting lysosomal alkalinization and impaired degradation in fresh and cultured RPE cells: evidence for a role in retinal degenerations. *Exp. Eye Res.* **126,** 68–76
32. Matsui, T., and Fukuda, M. (2014) Methods of analysis of the membrane trafficking pathway from recycling endosomes to lysosomes. *Methods Enzymol.* **534,** 195–206
33. Esteve-Rudd, J., Lopes, V. S., Jiang, M., and Williams, D. S. (2014) *In vivo* and *in vitro* monitoring of phagosome maturation in retinal pigment epithelium cells. *Adv. Exp. Med. Biol.* **801,** 85–90
34. Wavre-Shapton, S. T., Meschede, I. P., Seabra, M. C., and Futter, C. E. (2014) Phagosome maturation during endosome interaction revealed by partial rhodopsin processing in retinal pigment epithelium. *J. Cell Sci.* **127,** 3852–3861
35. Rakoczy, P. E., Lai, C. M., Baines, M., Di Grandi, S., Fitton, J. H., and Constable, I. J. (1997) Modulation of cathepsin D activity in retinal pigment epithelial cells. *Biochem. J.* **324,** 935–940
36. Regan, C. M., de Grip, W. J., Daemen, F. J., and Bonting, S. L. (1980) Degradation of rhodopsin by a lysosomal fraction of retinal pigment epithelium: biochemical aspects of the visual process: XLI. *Exp. Eye Res.* **30,** 183–191
37. Cingle, K. A., Kalski, R. S., Bruner, W. E., O'Brien, C. M., Erhard, P., and Wyszynski, R. E. (1996) Age-related changes of glycosidases in human retinal pigment epithelium. *Curr. Eye Res.* **15,** 433–438
38. Plantner, J. J., Le, M. L., and Kean, E. L. (1991) Enzymatic deglycosylation of bovine rhodopsin. *Exp. Eye Res.* **53,** 269–274
39. Finnemann, S. C. (2003) Focal adhesion kinase signaling promotes phagocytosis of integrin-bound photoreceptors. *EMBO J.* **22,** 4143–4154
40. Shelby, S. J., Colwill, K., Dhe-Paganon, S., Pawson, T., and Thompson, D. A. (2013) MERTK interactions with SH2-domain proteins in the retinal pigment epithelium. *PLoS ONE* **8,** e53964
41. Strick, D. J., Feng, W., and Vollrath, D. (2009) Mertk drives myosin II redistribution during retinal pigment epithelial phagocytosis. *Invest. Ophthalmol. Vis. Sci.* **50,** 2427–2435
42. Yao, J., Jia, L., Shelby, S. J., Ganios, A. M., Feathers, K., Thompson, D. A., and Zacks, D. N. (2014) Circadian and noncircadian modulation of autophagy in photoreceptors and retinal pigment epithelium. *Invest. Ophthalmol. Vis. Sci.* **55,** 3237–3246
43. Bulloj, A., Duan, W., and Finnemann, S. C. (2013) PI 3-kinase independent role for AKT in F-actin regulation during outer segment phagocytosis by RPE cells. *Exp. Eye Res.* **113,** 9–18
44. Laniosz, V., Holthusen, K. A., and Meneses, P. I. (2008) Bovine papillomavirus type 1: from clathrin to caveolin. *J. Virol.* **82,** 6288–6298
45. Querbes, W., O'Hara, B. A., Williams, G., and Atwood, W. J. (2006) Invasion of host cells by JC virus identifies a novel role for caveolae in endosomal sorting of noncaveolar ligands. *J. Virol.* **80,** 9402–9413
46. Matsui, T., Itoh, T., and Fukuda, M. (2011) Small GTPase Rab12 regulates constitutive degradation of transferrin receptor. *Traffic* **12,** 1432–1443
47. del Pozo, M. A., Balasubramanian, N., Alderson, N. B., Kiosses, W. B., Grande-García, A., Anderson, R. G., and Schwartz, M. A. (2005) Phosphocaveolin-1 mediates integrin-regulated membrane domain internalization. *Nat. Cell Biol.* **7,** 901–908
48. Lajoie, P., Goetz, J. G., Dennis, J. W., and Nabi, I. R. (2009) Lattices, rafts, and scaffolds: domain regulation of receptor signaling at the plasma membrane. *J. Cell Biol.* **185,** 381–385
49. Li, J., Scherl, A., Medina, F., Frank, P. G., Kitsis, R. N., Tanowitz, H. B., Sotgia, F., and Lisanti, M. P. (2005) Impaired phagocytosis in caveolin-1 deficient macrophages. *Cell Cycle* **4,** 1599–1607
50. Chang, Y., and Finnemann, S. C. (2007) Tetraspanin CD81 is required for the αvβ5-integrin-dependent particle-binding step of RPE phagocytosis. *J. Cell Sci.* **120,** 3053–3063
51. Shi, Y., Tan, S. H., Ng, S., Zhou, J., Yang, N. D., Koo, G. B., McMahon, K. A., Parton, R. G., Hill, M. M., Del Pozo, M. A., Kim, Y. S., and Shen, H. M. (2015) Critical role of CAV1/caveolin-1 in cell stress responses in human breast cancer cells via modulation of lysosomal function and autophagy. *Autophagy* **11,** 769–784
52. Shiroto, T., Romero, N., Sugiyama, T., Sartoretto, J. L., Kalwa, H., Yan, Z., Shimokawa, H., and Michel, T. (2014) Caveolin-1 is a critical determinant of autophagy, metabolic switching, and oxidative stress in vascular endothelium. *PLoS ONE* **9,** e87871
53. Kim, J. Y., Zhao, H., Martinez, J., Doggett, T. A., Kolesnikov, A. V., Tang, P. H., Ablonczy, Z., Chan, C. C., Zhou, Z., Green, D. R., and Ferguson, T. A. (2013) Noncanonical autophagy promotes the visual cycle. *Cell* **154,** 365–376
54. Martinez, J., Almendinger, J., Oberst, A., Ness, R., Dillon, C. P., Fitzgerald, P., Hengartner, M. O., and Green, D. R. (2011) Microtubule-associated protein 1 light chain 3 α (LC3)-associated phagocytosis is required for the efficient clearance of dead cells. *Proc. Natl. Acad. Sci. U.S.A.* **108,** 17396–17401
55. Mundy, D. I., Li, W. P., Luby-Phelps, K., and Anderson, R. G. (2012) Caveolin targeting to late endosome/lysosomal membranes is induced by perturbations of lysosomal pH and cholesterol content. *Mol. Biol. Cell* **23,** 864–880